Performance comparison of screen-printed piezoelectric structures on porous PZT and alumina substrates

Pierre Marechal, D. Kuscer, Franck Levassort, Louis Pascal Tran-Huu-Hue, Janez Holc, Marija Kosec, Marc Lethiecq

Performance comparison of screen-printed piezoelectric structures on porous PZT and alumina substrates

P. Maréchal[1], D. Kuščer[2], F. Levassort[1], L.P. Tran-Huu-Hue[1], J. Holc[2], M. Kosec[2], M. Lethiecq[1]

[1] François-Rabelais University, LUSSI, 10 boulevard Tonnellé, BP 3223, 37032 Tours cedex 1, France
[2] Joseph Stefan Institute, Jamova 39, Ljubljana, Slovenia
marechal@univ-tours.fr

***Abstract* — In previous work, screen-printing technology was used to elaborate an integrated piezoelectric structure on a porous substrate [1]. The substrate was chosen to withstand the film sintering temperature which was lowered at 800°C thanks to the addition of PGO to a PZT composition. The acoustical impedance of this substrate is very close to that of the deposited piezoelectric thick film, making it an adequate backing to deliver a short pulse-echo response, but the resonance frequency is lowered. Intermediate functional layers were necessary between the substrate and the piezoelectric layer. The transducer based on a porous PZT structure including a dense barrier layer and a gold rear electrode is used as a reference device. Here, another set of materials is considered as possible candidate to fulfill both functions of substrate and backing: porous alumina associated with a dense alumina barrier layer and platinum rear electrode. Since the thicknesses of these layers is not negligible compared to the wavelength of the first thickness mode of the piezoelectric layer, they have a relatively strong influence on the electro-acoustic response. The input acoustic impedance of this stack must be controlled very precisely in order to make it an adequate backing. The damping of the backing is optimized to deliver a relatively short pulse-echo response, without excessive lowering of the resonance frequency. The piezoelectric thick film on alumina substrate has similar properties to the one on porous PZT. A mean thickness around 30 micrometers and a thickness coupling factor around 40% were obtained in both cases. As a result of the damping, the structure resonates at 40 MHz, the anti-resonance of the piezoelectric thick film alone being around 65 MHz. Pulse-echo measurements allows comparison of the performance of the two devices in terms of sensitivity, axial resolution and bandwidth. The results are compared and discussed, showing that the sensitivity/bandwidth trade-offs of the two transducers are significantly different.**

I. Introduction

For high resolution ultrasound imaging, the materials constituting the piezoelectric transducer are to be chosen and designed in very low thicknesses. In the literature, a wide range of piezoelectric materials and fabrication processes [2-3] were used to build focused high frequency transducers.

Bulk properties of constitutive materials are well known, but they are often modified according to the fabrication process and surrounding layer properties. Particularly, the electro-mechanical properties of the piezoelectric layer are strongly dependent on the porosity level. Here, the functional layers are deposited using a screen-printing process on a substrate used as a backing [1].

In part II, the fabrication process of materials constituting the integrated screen-printed transducer is presented. Then, in part III, the electro-mechanical properties of two samples of PZT/PGO structures on porous alumina are compared. The properties of the layers constituting the PZT/PGO transducers are then characterized. In part IV, the performance of PZT/PGO transducers is characterized and results compared with modeling.

II. Fabrication

The manufacture of the integrated structure is described, from the development of the substrate to the screen-printing deposition of the piezoelectric layer, including a barrier layer in order to limit the diffusion in the substrate during the sintering, a front and a back electrode. The main specificity of this structure is its porous substrate withstanding the sintering temperature necessary for the screen-printed layers.

A. Porous substrate

The substrate material was selected for its ability to withstand the sintering temperature, its chemical neutrality, and its moderate acoustic impedance. Thus, the range of available material is limited among porous metal oxides. In this study, a transducer based on porous Al_2O_3 substrate is compared to the reference porous PZT substrate. To fabricate the porous Al_2O_3, a mix of fine (Alcoa A–16, 99%) and coarse (Alcoa CL 3000) alumina powders was used. This mix was sintered at 1450°C for 2 hours. This material was formed without pore-formers. Once fabricated, the substrate micro-structure was analyzed and characterized by a scanning electron microscope (SEM Jeol 5800) equipped by energy dispersive spectroscopy system (EDS). The volume fraction of porosity was measured at v_f = 14% and v_f = 16% for porous PZT and porous Al_2O_3, respectively (Fig. 1).

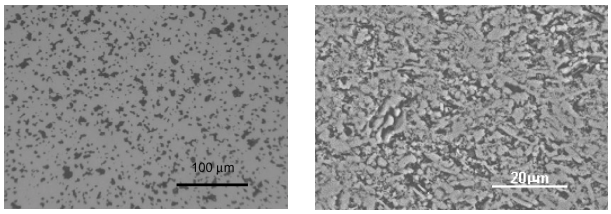

(a) (b)

Fig. 1: Micro-structure of (a) porous PZT and (b) porous Al_2O_3.

The effective acoustic properties of porous PZT ceramic and porous Al_2O_3 were deduced considering them as 3-0 connectivity composites (closed porosity) and using an homogenization model [4]. The evaluated longitudinal wave velocity was corroborated by a time-of-flight measurements and the density was confirmed using Archimedes method (TABLE I).

TABLE I: ACOUSTIC PROPERTIES OF POROUS SUBSTRATES.

Substrate	v_f (%)	ρ (kg/m^3)	c_l (m/s)	Z (MRa)	α (dB/mm/MHz)
Porous PZT	14	6660	2730	18.2	0.26
Porous Al_2O_3	16	3300	5900	19.5	0.15

v_f: volume fraction of porosity; ρ:density; c_l: longitudinal wave velocity; Z: acoustic impedance; α: attenuation coefficient.

B. Screen-printed layers

The screen-printing process is then used to deposit functional layers. It consists in scraping on a grid a fine layer of ink made up of constitutive metallic oxides mixed with an organic binder and a solvent. After each screen-printing deposition, the ink is dried. Since the substrate is porous, diffusion of the rear electrode was observed during the sintering. Therefore, it was necessary to add an intermediate dense barrier layer to avoid diffusivity and formation of undesirable phases. Several passes of paste of the same material as for the substrate were deposited without any pore former. Then, the rear electrode can be deposited with less diffusion. Nevertheless, a particular attention is to be paid to this barrier layer since its acoustic impedance is higher than that of the substrate. For this Al_2O_3 based structure, a paste was prepared from fine Al_2O_3 powder (Alcoa A 16), printed in two passes and sintered at 1400°C for 2 hours. The rear electrode was formed either with Pt or Au. In the case of a Pt rear electrode, it is made of Pt unfritted paste, printed in two passes and sintered at 1200°C for 2 hours. When a Au rear electrode is tested, it is made of Au fritted paste, printed in two passes and sintered at 850°C for 2 hours. For all samples, the PZT film doped with 2% of PGO was deposited in 5 passes, sintered at 800°C for 8 h under a PbO rich atmosphere. The front gold electrode was then sputtered. Finally, the PZT/PGO film was poled in an oil bath at 160°C for 5 minutes and cooled down to room temperature, under an electric field of 3 kV/mm.

III. CHARACTERIZATION

The electrical, acoustic and electro-mechanical parameters of the thickness mode were identified on the basis of preliminary thicknesses evaluation.

A. Thickness and density

A SEM cross-section photograph of the integrated structures was performed (Fig. 2). The mean thickness t and the porosity level v_f were estimated for each layer from the cross-section images. The acoustic properties of a passive layer are characterized by its acoustic impedance $Z = \rho c_l$ and angular delay $\theta = 2\pi ft/c_l$. Thus, the number of unknown variables is reduced to the longitudinal wave velocity c_l, which was fitted and corroborated by an homogenization model [4].

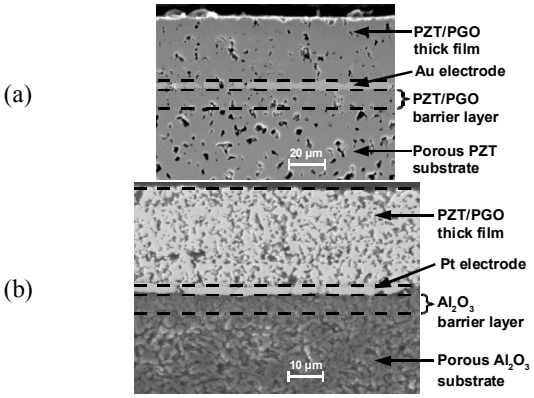

Fig. 2: SEM photograph of a PZT/PGO integrated structure (a) on porous PZT substrate and (b) on porous Al2O3 substrate.

The porosity and the related density were determined by stereological analysis as for the porous PZT substrate. On the basis of previous studies, the density was increased by adding PbO powder during the sintering process. The corresponding volume fraction was evaluated around $v_f = 11\%$ and $v_f = 10\%$, the density of the piezoelectric thick film was deduced $\rho = 6900$ kg/m^3 and $\rho = 7000$ kg/m^3, for the structure based on porous PZT substrate and porous Al_2O_3 substrate, respectively. Since the electrodes were considered to be pure metals, the acoustic properties of these layers were imposed.

B. Electro-mechanical properties

The complex electrical impedance was measured as a function of frequency $Z_e(f)$ around the fundamental thickness-mode resonance of the integrated structure. Using the thickness and density measurements (Fig. 2), the KLM model was used to simulate and fit the electrical impedance of this five layer structure (substrate, barrier layer, back electrode, piezoelectric thick film, front electrode). The obtained properties for constitutive layers are summarized in TABLE II.

TABLE II: LAYER PROPERTIES OF THE INTEGRATED STRUCTURES.

Substrate	Porous PZT		Porous Al_2O_3	
Property	Z (MRa)	t (μm)	Z (MRa)	t (μm)
Front electrode	63.8	0.5	63.8	0.1
Piezoelectric film	29.8	32	29.2	33
Back electrode	63.8	5	69.8	8
Barrier layer	24.0	12	23.4	10
Substrate	18.2	10000	19.5	12000

Z: acoustic impedance; t: thickness.

Therefore, missing parameters concerning the piezoelectric thick film were fitted (longitudinal wave velocity c_l, thickness coupling factor k_t, dielectric constant at constant strain $\varepsilon_{33}^S/\varepsilon_0$ and mechanical losses δ_m). The electro-mechanical properties are summarized in TABLE III. Knowing the piezoelectric layer thickness variations t_p = 33±3 μm for the sample based on porous Al_2O_3 substrate (Fig. 2 (b)), the accuracy of each fitted parameter was quantified. The longitudinal wave velocity c_l = 4170±120 m/s the thickness coupling factor k_t = 37±2%, the dielectric constant at constant strain $\varepsilon_{33}^S/\varepsilon_0$ = 700±40, dielectric and mechanical losses δ_e = 2±2% and δ_m = 5±1.5% appeared to be reliable [3].

TABLE III: ELECTROMECHANICAL PROPERTIES OF THE PIEZOELECTRIC THICK FILM.

Substrate	Z (MRa)	ρ (kg/m^3)	c_l (m/s)	k_t (%)	$\frac{\varepsilon_{33}^S}{\varepsilon_0}$	δ_m (%)	δ_e (%)
Porous PZT	29.8	6900	4300	41	510	22	0.5
Porous Al_2O_3	29.2	7000	4170	37	700	5	1.0

Z: acoustic impedance; ρ: density; c_l: longitudinal wave velocity; k_t: thickness coupling coefficient; $\varepsilon_{33}^S/\varepsilon_0$: relative dielectric constant; δ_m and δ_e: mechanical and dielectric losses.

The fitted experimental electrical impedance of the integrated structure is represented for the two PZT/PGO samples on porous PZT substrate (Fig. 3 (a) and (b)) and on porous Al_2O_3 substrate (Fig. 3 (c) and (d)). It must be noticed that the anti-resonance peak ($\lambda/2$ first thickness mode), f_a = 67 and 65 MHz, respectively, is lowered and damped due to the integrated structure in comparison with that of a free piezoelectric plate. Indeed, the resonance frequency is nearly the same for both integrated structures, i.e. f_0 = 42 and 40 MHz, respectively. Even if these resonance characteristics are nearly the same, the bandwidth clearly appears to be related to the thickness and acoustic properties of the back electrode and barrier layer. These layers are essential in the electrical and chemical point of view for the piezoelectric structure, but they can significantly lower the resonance frequency or the bandwidth of the integrated structure. Moreover, their thickness and acoustic properties are difficult to control precisely, due to the fabrication process.

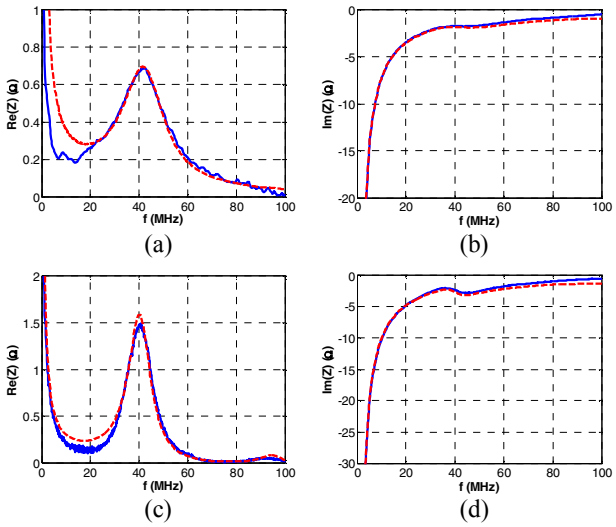

Fig. 3: Experimental (solid) and simulated (dashed) (a), (c) real and (b), (d) imaginary parts of the fitted electrical impedance $Z_e(f)$ of PZT/PGO integrated structure screen-printed on (a), (b) porous PZT substrate and (c), (d) porous Al_2O_3 substrate.

IV. TRANSDUCER

A. Characterization

Before the finalization of the transducers, back and front electrodes of the integrated structure are connected to an electrical cable. Then, they are connected to a high frequency home-made pulse generator, and their electro-acoustic response is measured and compared with simulation (Fig. 4).

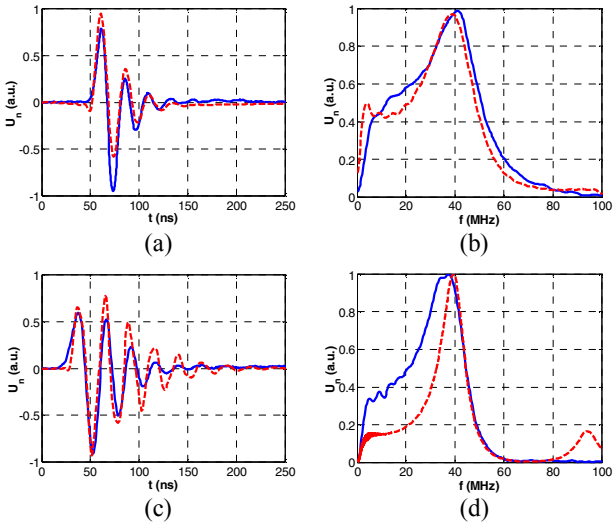

Fig. 4: Comparison of the normalized electro-acoustic response obtained in water by experiment (solid) and KLM simulation (dashed) as a function of (a), (c) time and (b), (d) frequency for the integrated structure screen-printed on (a), (b) porous PZT substrate and (c), (d) porous Al_2O_3 substrate.

There is a good agreement for the sample based on a porous PZT substrate (Fig. 4 (a) and (b)), but for that based on a porous Al_2O_3 substrate (Fig. 4 (c) and (d)), the comparison between experiment and simulation is not so satisfactory. This disagreement could be due to reproducibility since the layers thicknesses were evaluated on a different sample. Characterization results are summarized in TABLE IV and compared between the two transducers. Even if their structure is very similar, their echo and spectrum are very different: the bandwidth of the porous Al_2O_3 based structure is significantly reduced and the sensitivity is –6 dB lower compared to that of the porous PZT based structure. As a result, the axial resolution is more than twice lower.

TABLE IV: EXPERIMENTAL TIME AND FREQUENCY CHARACTERISTICS MEASURED IN PULSE-ECHO MODE ON A FLAT TARGET

Substrate	f_0 (MHz)	f_6 (MHz)	$BW_{6,r}$ (%)	Δz_6 (µm)	S (dB)
Porous PZT	40	31	124	15	0
Porous Al_2O_3	37	33	73	34	–6

f_0: resonance frequency; f_6: low cut-off frequency at –6 dB; $BW_{6,r}$: relative bandwidth; Δz_6: axial resolution; S: relative sensitivity.

B. *Influence of the rear layers*

Since the front face is only made of a thin layer of gold for both samples, its influence on the resulting piezoelectric resonance can be neglected. Therefore, the observed resonance could be explained by the properties of the resonator at the rear face of the piezoelectric layer, which is made of the rear electrode, the barrier layer and the porous substrate. Indeed, the input impedance of the back face of the piezoelectric layer $Z_{in,back}$ has an influence on the resonance [5]. As the thickness of the back electrode grows (Fig. 5 (a)), the normalized input impedance of the back face of the piezoelectric layer $|Z_{in,back}|/|Z_p|$ increases at the resonance frequency from 1 to 6. At higher frequency, the ratio $|Z_{in,back}|/|Z_p|$ reaches 10, resulting in a nearly perfect reflection. This increasing reflection by the rear layers results in a longer –6 dB duration estimated both on the echo and deduced from the bandwidth using the well-known relationship for gaussian envelopes (Fig. 5 (b)).

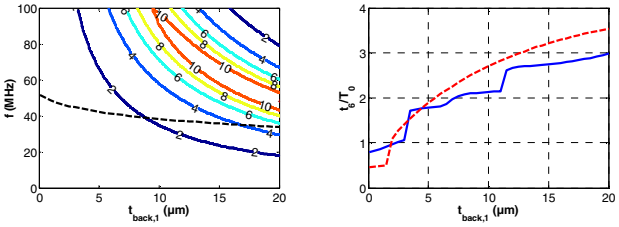

(a) (b)

Fig. 5: (a) Isovalues of the modulus of the normalized back input impedance $|Z_{in,back}|/|Z_p|$ and resonance frequency f_0 (dashed line) for the Al_2O_3 based structure as a function of the thickness of the rear electrode $t_{back,1}$ and frequency f. (b) Normalized –6 dB echo duration for the Al_2O_3 based structure, where $T_0 = 1/f_0$ as a function of the thickness of the rear electrode $t_{back,1}$ (solid line) evaluated on the echo and deduced from the bandwidth $BW_{6,r}$ (dashed line).

$$\frac{t_6}{T_0} = \frac{4\log(2)}{\pi.BW_{6,r}} \approx \frac{0.88}{BW_{6,r}}$$

In that case, the optimum thickness of the rear electrode would be as small as possible (similarly for the barrier layer). Nevertheless, due to the fabrication process, particularly the sintering of upper layers, it is difficult to make it thiner than 5 µm, or else it no longer guarantees electrical conduction. In that case, the axial resolution would be improved but not dramatically.

V. CONCLUSION

In this study, two integrated transducers were compared: one was based on a porous PZT substrate, the second was based on a porous Al_2O_3 substrate. Their structures were very similar, but their performance was significantly different. It was highlighted that not only the material properties was an important parameter, but also the thickness itself and its homogeneity. These properties are closely linked to the screen-printing process, which imposes a minimum thickness for each functional layer. This involves some perturbations in the resonance spectrum and could result in a reduced bandwidth compared to that of a well damped resonance as for the reference transducer based on a porous PZT substrate. For the porous Al_2O_3-based structure, the characteristics are slightly lower (in terms of sensitivity and axial resolution) than those of the porous PZT based structure. The main reasons are a lower thickness coupling factor, higher thickness of the bottom electrode and higher acoustic impedance of the substrate for the Al_2O_3 structure.

ACKNOWLEDGMENT

This work was funded by the EU through the FP6 NoE MIND. The authors would like to thank Jean-Yves Tartu for transducer manufacturing, and Jean-Marc Grégoire for transducer characterization.

REFERENCES

1. Maréchal P., Levassort F., Holc J., Tran-Huu-Hue L.P., Kosec M., Lethiecq M., *High-frequency transducers based on integrated piezoelectric thick films for medical imaging,* IEEE Transactions on Ultrasonics, Ferroelectrics and Frequency Control, 2006. **53**(8): p.1524-1533.
2. Foster F.S., Harasiewicz K.A., Sherar M.D., *A history of medical and biological imaging with PVDF transducers*, IEEE Transactions on Ultrasonics, Ferroelectrics and Frequency Control, 2000. **47**(6): p.1363-1371.
3. Cannata J.M., Ritter T.A., Chen W.C., Silverman R.H., Shung K.K., *Design of efficient, broadband single-element (20-80 MHz) ultrasonic transducers for medical imaging applications*, IEEE Transactions on Ultrasonics, Ferroelectrics and Frequency Control, 2003. **50**(11): p.1548-1557.
4. Levassort F., Holc J., Ringgaard E., Bove T., Kosec M., Lethiecq M., *Fabrication, modelling and use of porous ceramics for ultrasonic transducer applications*, Journal of Electroceramics, 2007. **19**(1) , p.125-137.
5. Lee S.H., Yoon K.H., Lee J.K., *Influence of electrode configurations on the quality factor and piezoelectric coupling constant of solidly mounted bulk acoustic wave resonators*, Journal of Applied Physics, 2002. **92**(7): p.4062-4069.